Polyethylenimine-based siRNA nanocomplexes reprogram tumor-associated dendritic cells via TLR5 to elicit therapeutic antitumor immunity

Juan R. Cubillos-Ruiz,[1] Xavier Engle,[1] Uciane K. Scarlett,[1] Diana Martinez,[1] Amorette Barber,[1] Raul Elgueta,[1] Li Wang,[1] Yolanda Nesbeth,[1] Yvon Durant,[2] Andrew T. Gewirtz,[3] Charles L. Sentman,[1] Ross Kedl,[4] and Jose R. Conejo-Garcia[1,5]

[1]Department of Microbiology and Immunology, Dartmouth Medical School, Lebanon, New Hampshire, USA. [2]Nanostructured Polymers Research Center, University of New Hampshire, Durham, New Hampshire, USA. [3]Department of Pathology, Emory University, Atlanta, Georgia, USA. [4]Department of Immunology, University of Colorado, Denver, Colorado, USA. [5]Department of Medicine, Dartmouth Medical School, Lebanon, New Hampshire, USA.

The success of clinically relevant immunotherapies requires reversing tumor-induced immunosuppression. Here we demonstrated that linear polyethylenimine-based (PEI-based) nanoparticles encapsulating siRNA were preferentially and avidly engulfed by regulatory DCs expressing CD11c and programmed cell death 1–ligand 1 (PD-L1) at ovarian cancer locations in mice. PEI-siRNA uptake transformed these DCs from immunosuppressive cells to efficient antigen-presenting cells that activated tumor-reactive lymphocytes and exerted direct tumoricidal activity, both in vivo and in situ. PEI triggered robust and selective TLR5 activation in vitro and elicited the production of hallmark TLR5-inducible cytokines in WT mice, but not in *Tlr5*–/– littermates. Thus, PEI is a TLR5 agonist that, to our knowledge, was not previously recognized. In addition, PEI-complexed nontargeting siRNA oligonucleotides stimulated TLR3 and TLR7. The nonspecific activation of multiple TLRs (specifically, TLR5 and TLR7) reversed the tolerogenic phenotype of human and mouse ovarian tumor–associated DCs. In ovarian carcinoma–bearing mice, this induced T cell–mediated tumor regression and prolonged survival in a manner dependent upon myeloid differentiation primary response gene 88 (MyD88; i.e., independent of TLR3). Furthermore, gene-specific siRNA-PEI nanocomplexes that silenced immunosuppressive molecules on mouse tumor-associated DCs elicited discernibly superior antitumor immunity and enhanced therapeutic effects compared with nontargeting siRNA-PEI nanocomplexes. Our results demonstrate that the intrinsic TLR5 and TLR7 stimulation of siRNA-PEI nanoparticles synergizes with the gene-specific silencing activity of siRNA to transform tumor-infiltrating regulatory DCs into DCs capable of promoting therapeutic antitumor immunity.

Introduction

Despite significant advances in cancer cell biology, the survival rate for patients with some of the most aggressive and frequent epithelial tumors, such as ovarian or pancreatic cancer, has improved very little in the last 30 years (1). Aggressive epithelial cancers evolve not only to escape from spontaneous protective immunity, but also to use the inflammatory machinery for abrogating the immune mechanisms that exert natural immune pressure against cancer progression (2–5). As we start understanding the peculiarities of the immunosuppressive microenvironment of these tumors, promising therapeutic targets are emerging. Some potentially targetable immunosuppressive mechanisms commonly orchestrated by epithelial cancers include the accumulation of regulatory T lymphocytes (6) and myeloid-derived suppressor cells (4). Additionally, tumors often employ the overexpression of immunosuppressive programmed cell death 1–ligand 1 (PD-L1) as

a mechanism of immune evasion (3, 7). In fact, antibody blockade of PD-L1 on monocyte-derived DCs generated from cancer ascites improves T cell–mediated antitumor responses (3), implicating in vivo neutralization of PD-L1 as a therapeutic goal.

While most aggressive epithelial tumors use common immunosuppressive mediators, different microenvironmental signals determine the predominance of distinct tolerogenic mechanisms in different histological types of cancer. Thus, our recent work about the microenvironment of ovarian cancer, a paradigmatic lethal and frequent form of epithelial cancer, demonstrated that immature CD11c+DEC205+ DCs represent the most frequent leukocyte subset infiltrating solid tumors (2, 8–13). These DCs home to perivascular locations, where they deliver multiple proangiogenic (2, 8–12) and immunosuppressive (2, 13) mediators. Correspondingly, we recently demonstrated that the elimination of such tumor-associated DCs delays ovarian cancer progression by boosting antitumor immunity (13). Thus, it is likely that the release of this crucial immunosuppressive brake enables the awakening of tumor-infiltrating effector lymphocytes, the only known element of the ovarian carcinoma microenvironment capable of exerting spontaneous immune pressure against tumor progression (12, 14, 15).

Although regulatory DCs at tumor locations take up tumor materials (9), they express very low MHC and costimulatory mol-
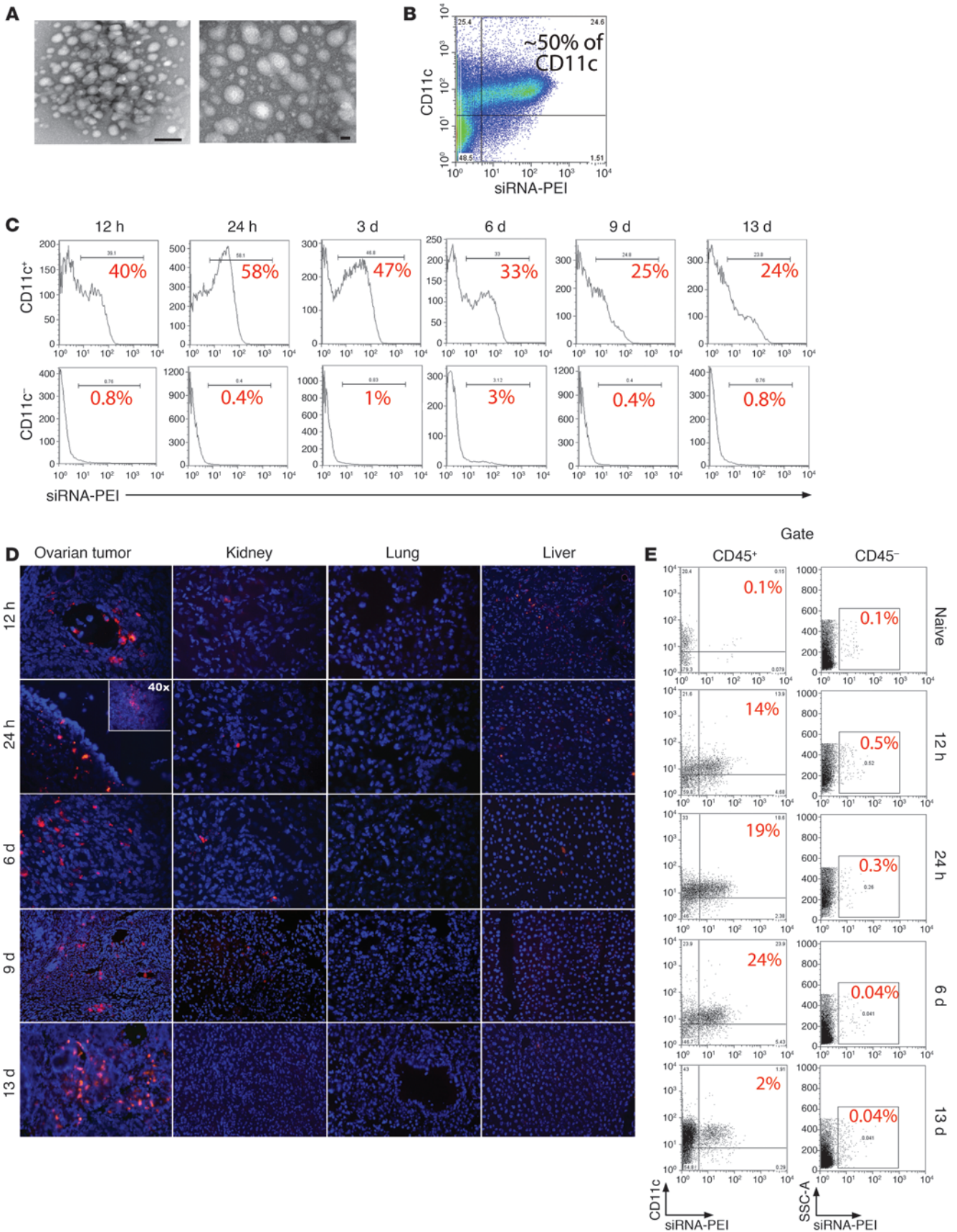
Figure 1

siRNA-PEI nanoparticles are preferentially engulfed by tumor-associated DCs. (**A**) NTsiRNA-PEI were stained with uranyl acetate and visualized using transmission electron microscopy. Original magnification, ×145,000 (left); ×285,000 (right). Scale bars: 20 nm (left); 100 nm (right). Average nanoparticle size was 40–60 nm. (**B**) Selective engulfment of NTsiRNA-PEI by peritoneal tumor-associated CD11c$^+$ DCs. Rhodamine-labeled NTsiRNA-PEI were intraperitoneally injected into mice bearing ID8-*Defb29/Vegf-A* ovarian carcinoma, and peritoneal wash samples were analyzed by FACS after 3 days. (**C**) Time-course analysis of nanocomplex uptake by peritoneal CD11c$^+$ DCs in tumor-bearing mice after a single intraperitoneal injection. The percentage of cells retaining the nanoparticles is indicated for each time point. Data are representative of 3 mice analyzed per time point in 2 independent experiments. (**D**) Biodistribution of intraperitoneally injected siRNA-PEI nanoparticles. Ovarian carcinoma–bearing mice received a single intraperitoneal injection of rhodamine-labeled NTsiRNA-PEI, and multiple organs were collected at different time points after injection. Fluorescence microscopy was performed on histological sections from different organs to determine the presence of nanoparticles. Red indicates rhodamine-labeled nanocomplexes. Blue denotes nuclei. Data are representative of at least 3 independent experiments. Original magnification, ×200; ×40 (inset). (**E**) Nanoparticle uptake by DCs infiltrating solid ovarian tumors. Ovaries from tumor-bearing mice were collected at different time points after a single intraperitoneal injection with rhodamine-labeled NTsiRNA-PEI. Shown is the percentage of ovarian tumor–resident DCs engulfing nanoparticles in situ, determined by FACS. Data are representative of 2 independent experiments. SSC-A, side-scattered light.

ecules (13); however, their capacity to efficiently present antigens can be promoted in a less suppressive microenvironment (9). Therefore, transforming tumor-associated DCs from an immunosuppressive to an immunostimulatory cell type in vivo and in situ theoretically represents a doubly effective therapeutic approach that combines the advantages of classical immunostimulatory DC-based vaccine strategies and the beneficial effects of removing this tolerogenic component.

Recent reports have attributed the therapeutic effects of in vivo–delivered siRNA oligonucleotides in successful clinical trials to the nonspecific activation of TLR7 (16) or TLR3 (17, 18). This intrinsic immunostimulatory capacity (19, 20) has raised major concerns about the feasibility of specifically silencing precise gene targets, but also opens major opportunities for reversing immunosuppressive mechanisms commonly orchestrated by tumors while synergistically silencing crucial immunosuppressive determinants. Even though seminal studies by Sood and colleagues have successfully silenced genes expressed by ovarian tumor cells in vivo (21–23), tumor-associated leukocytes with antitumor potential have never been targeted. Because of the phagocytic capacity of immature DCs at tumor locations (9, 13), the persistent silencing caused by nonviral siRNA in the absence of multiple cell divisions (24), and the intrinsic immunostimulatory activity of siRNA (16, 17), we hypothesized that nanocomplexes delivering siRNA against immunosuppressive determinants could reverse the regulatory activity of tumor DCs and promote their capacity to act as Trojan horses that efficiently present the tumor antigens that they have taken up in the tumor microenvironment.

Here we show that nanoparticles of linear polyethylenimine (PEI) and siRNA (referred to herein as siRNA-PEI nanoparticles) were selectively engulfed by tumor-associated DCs in vivo that, because of the intrinsic immunostimulatory activity of their vari-

ous components, enhance antigen-presenting capacity and induce direct tumoricidal activity independently of the siRNA sequence. Moreover, delivering siRNA specific for immunosuppressive determinants persistently downregulated these molecules in vivo and therefore induced discernible superior therapeutic effects. Our results underscore the feasibility of reprogramming tumor-associated regulatory DCs in situ to elicit therapeutically relevant antitumor immune responses in aggressive ovarian carcinoma–bearing hosts, which may be applicable to other lethal epithelial cancers.

Results

siRNA-PEI nanoparticles are preferentially and avidly engulfed by tumor-associated DCs. Human and murine peritoneal ovarian carcinomas are heavily infiltrated by immunosuppressive DCs that phagocytose tumor materials (9, 13). To take advantage of their high frequency and phagocytic capacity, we first defined an optimal carrier that could deliver stabilized siRNA after preferential engulfment by tumor-associated DCs. Anti-CD11c antibody–targeted zwitterionic liposomes did not successfully stabilize the siRNA or failed to deliver it effectively to tumor DCs (Supplemental Figure 1; supplemental material available online with this article; doi:10.1172/JCI37716DS1). In contrast, linear PEI, an endotoxin-free, cationic polymer that protects siRNA from degradation (25, 26), formed stable nanocomplexes of approximately 50 nm with 21-nucleotide siRNA (Figure 1A) that were preferentially and avidly engulfed by CD11c$^+$ DCs at tumor locations (Figure 1B). Notably, selective uptake of rhodamine-labeled siRNA-PEI nanocomplexes by regulatory tumor DCs took place in the absence of targeting motifs, while less than 1% of tumor cells or other leukocytes at tumor locations incorporated the nanoparticles (Supplemental Figure 2A). Nanoparticles were engulfed as quickly as 12 hours after intraperitoneal injection and were preferentially retained by peritoneal tumor DCs for up to 13 days (Figure 1C). Consistent with the massive homing of CD11c$^+$ regulatory DCs specifically to solid ovarian cancers (9, 13), rhodamine-labeled siRNA-PEI nanoparticles were also primarily found in solid ovarian tumors beginning 12 hours after intraperitoneal injection, where they remained for at least 13 days (Figure 1D), selectively engulfed by tumor-infiltrating DCs but not other cell types (Figure 1E and Supplemental Figure 2B). Further supporting a selective and avid uptake by peritoneal tumor DCs, few nanoparticles were incorporated and retained for up to 13 days by splenic CD11c$^+$ DCs (less than 4%; Supplemental Figure 2, C and D), while scarce nanocomplexes were occasionally found in the kidney and liver, and none were detected in the lung at any temporal point (Figure 1D). Together, these data indicate that, even in the absence of specific targeting, siRNA-PEI nanocomplexes are preferentially and avidly engulfed by abundant phagocytic DCs at tumor locations.

siRNA-PEI nanocomplex uptake induces maturation of tumor-associated regulatory DCs. We next examined the phenotype of the tumor DCs that engulf and retain nanocomplexes in the tumor microenvironment. For that purpose, we first analyzed peritoneal wash samples from mice growing aggressive ID8-*Defb29/VEGF-A* tumors (9, 13) after a single intraperitoneal injection of either PBS or rhodamine-labeled PEI-based nanocomplexes encapsulating nontargeting 21-nt siRNA (NTsiRNA-PEI), with no homology to any rodent or human gene. Confirming our previous observations (9), tumor-associated CD11c$^+$ DCs in untreated hosts exhibited an immature phenotype, characterized by low expression of CD80 and MHC-II (Figure 2A). In
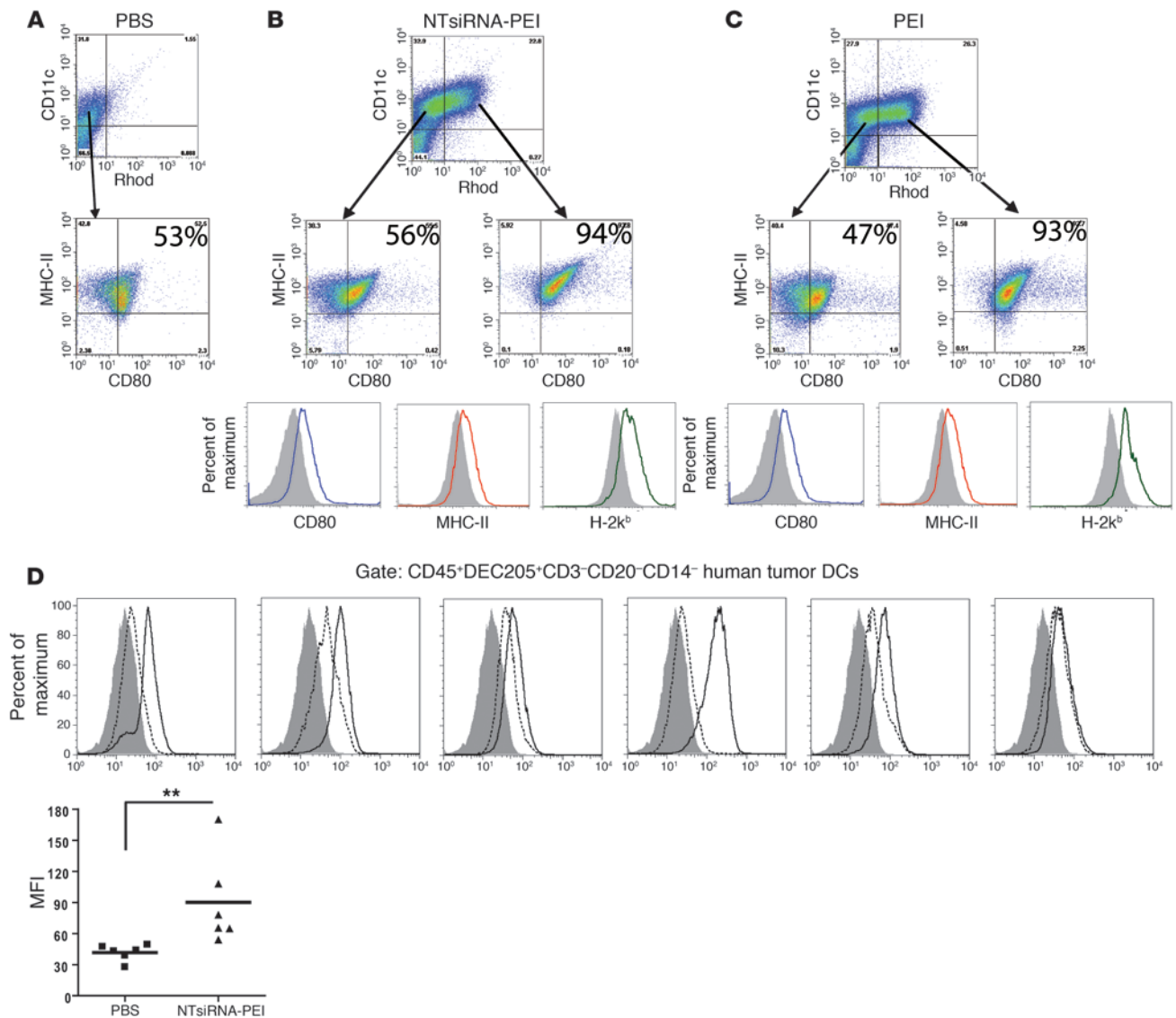
Figure 2
Engulfment of PEI-based nanocomplexes induces maturation of tumor-associated DCs in vivo and in situ. (**A**) Expression of CD80 and MHC-II on tumor-associated DCs from mice bearing ID8-*Defb29/Vegf-A* tumors for 3 weeks and injected with PBS. (**B**) Rhodamine-labeled NTsiRNA-PEI or (**C**) equivalent amounts of rhodamine-labeled PEI alone (see Methods) were intraperitoneally injected into mice bearing ID8-*Defb29/Vegf-A* tumors for 3 weeks. Expression of CD80, MHC-I, and MHC-II on tumor DCs that engulfed the nanoparticles or PEI was analyzed by FACS 3 days later. Rhod, rhodamine-labeled PEI. Filled histograms represent expression on DCs that did not engulf nanoparticles or PEI. Open histograms indicate expression by DCs that engulfed nanoparticles or PEI in the same host. Data are representative of 3 mice per group in 4 independent experiments. In **A**–**C**, the percentage of tumor-associated DCs coexpressing MHC-II and CD80 is indicated. (**D**) siRNA-PEI nanoparticles induced maturation of human tumor DCs. Leukocytes from 6 unselected dissociated stage III human ovarian tumors were enriched by Ficoll, 5×10^6 cells were incubated in 5 ml RPMI containing 100 μl PBS (dotted histograms) or 100 μl NTsiRNA-PEI (open histograms; see Methods), and the levels of CD80 on CD45+DEC205+CD3−CD20−CD14− tumor DCs were analyzed by FACS 18 hours later. Filled histograms represent staining with isotype control antibodies. MFI, mean fluorescence intensity of CD80 staining. Data points and horizontal bars denote individual values and means, respectively. **$P < 0.01$ (Mann-Whitney).

contrast, virtually all CD11c+ DCs engulfing NTsiRNA-PEI at tumor locations showed increased surface levels of CD80, MHC-I, and MHC-II 3 days after injection, compared with tumor DCs that did not incorporate nanoparticles in the same host (Figure 2B). Importantly, identical results were obtained when nanoparticles delivering a gene-specific 21-nt siRNA were injected (Supplemental Figure 3A).

Strikingly, we found that the cationic polymer used to complex the siRNA, PEI, was sufficient to mediate the upregulation of CD80, MHC-II, and MHC-I on tumor DCs in vivo (Figure 2C) in a manner dependent upon myeloid differentiation primary response gene 88 (MyD88; Supplemental Figure 3B), which suggests that siRNA-PEI nanocomplexes induce TLR signaling.

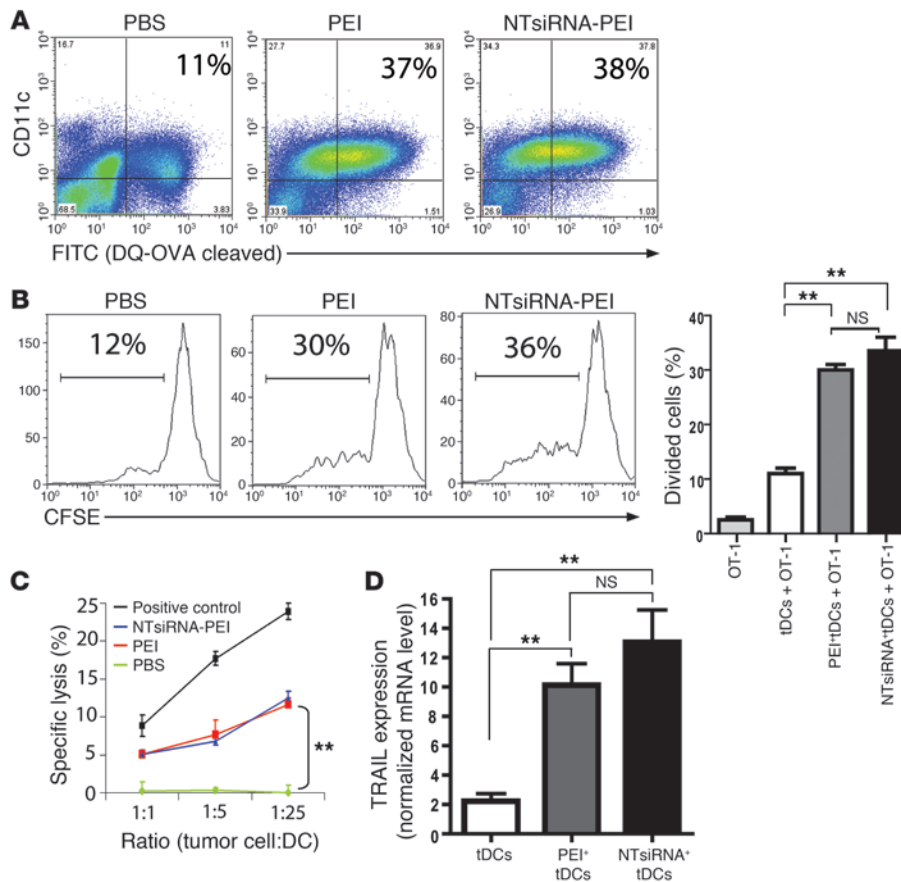To determine the clinical applicability of our findings, we incu-

Figure 3
siRNA-PEI nanoparticles enhance antigen presentation and induce tumoricidal activity by ovarian cancer DCs. (**A**) Improved antigen-processing capacity of tumor DCs engulfing PEI-based nanocomplexes in vivo. Mice bearing ID8-*Defb29/Vegf-A* tumors were intraperitoneally injected with DQ-OVA (see Methods), and 24 hours later received a single intraperitoneal injection of PBS, PEI, or NTsiRNA-PEI (3 mice per group, 2 independent experiments). Percentages denote the proportion of peritoneal tumor-associated DCs that efficiently processed the probe (FITC+), determined by FACS 48 hours later. (**B**) Enhanced antigen-presenting ability of OVA-pulsed tumor DCs (tDCs) engulfing siRNA-PEI nanoparticles in vivo (see Methods). Shown are representative FACS analysis of CFSE dilution and graphical representation of percent proliferating cells in triplicate for each condition. (**C**) Uptake of siRNA-PEI nanocomplexes induced tumoricidal DCs. Tumor-bearing mice were intraperitoneally injected with PBS, PEI, or NTsiRNA-PEI; 36 hours later, CD11c+MHC-II+CD3-NK1.1- tumor DCs from each group were sorted and incubated with ^{51}Cr-labeled ID8-*Defb29/Vegf-A* cells. Release of ^{51}Cr was measured in cell supernatants 5 hours later. Radiolabeled tumor cells were also cocultured with C57BL/6 splenocytes preincubated with 1,000 U/ml IL-2 for 5 days as a positive control of lysis. (**D**) Quantification of TRAIL mRNA levels by real-time RT-PCR in the same tumor DCs as in **C**. Error bars in **B**–**D** denote SEM. **$P < 0.01$.

based nanoparticles, upregulation of costimulatory CD80 was also induced on immature human monocyte-derived DCs treated with these nanocomplexes (Supplemental Figure 3D).

siRNA-PEI nanocomplexes enhance antigen presentation and induce cytotoxicity by tumor DCs. To determine whether immunostimulatory siRNA-PEI nanoparticles also influence the capacity of tumor-infiltrating DCs to process and present antigens, mice growing ID8-*Defb29/Vegf-A* ovarian tumors for 2 weeks were intraperitoneally injected with a self-quenched conjugate of OVA that exhibits green fluorescence upon proteolytic degradation; 24 hours later, these mice received a single intraperitoneal injection of PBS, PEI alone, or NTsiRNA-PEI ($n = 3$ per group; 2 independent experiments). After 48 hours, approximately 11% of peritoneal CD11c+ DCs had taken up and processed the OVA probe in PBS-injected mice. In contrast, mice injected with either PEI alone or NTsiRNA-PEI showed a 4-fold increase in the percentage of peritoneal CD11c+ DCs exhibiting green fluorescence ($P < 0.05$, Mann-Whitney test; Figure 3A), which indicates that tumor DCs engulfing siRNA-PEI nanoparticles process antigens more efficiently. Most importantly, CD45+CD11c+MHC-II+ DCs targeted by rhodamine-labeled PEI or rhodamine-labeled NTsiRNA-PEI in the peritoneal cavity of established ID8-*Defb29/Vegf-A* tumor–bearing mice, previously injected with full-length endotoxin-free OVA, induced a significantly stronger proliferation of CFSE-labeled OVA-specific OT-1 CD8+ T cells, compared to tumor DCs isolated from PBS-treated mice (Figure 3B). Together, these data indicate that engulfment of siRNA-PEI nanocomplexes enhances the antigen-presenting capacity of tolerogenic tumor DCs in vivo and in situ.

Because CD11c+ tumor DCs have previously been shown to acquire tumor-killing activity upon TLR stimulation (27, 28), we next determined whether PEI-based nanoparticles also induce the tumoricidal activity of ovarian cancer–infiltrating DCs. As expected, CD11c+MHC-II+NK1.1- DCs immunopurified from ID8-*Defb29/Vegf-A* tumor–bearing mice treated with PBS were incapable of lysing radiolabeled ID8-*Defb29/Vegf-A* ovarian carcinoma cells (Figure 3C). In contrast, as shown in Figure 3, C and D, tumor-derived CD11c+MHC-II+NK1.1- DCs sorted from mice injected with either PEI alone or NTsiRNA-PEI rapidly killed ID8-*Defb29/Vegf-A* tumor cells in a dose-dependent manner and dramatically upregulated expression of the TNF-related apoptosis-inducing ligand (TRAIL; refs. 27, 28). Together, our results indicate that NTsiRNA-PEI reprogram

bated multiple dissociated human ovarian carcinoma specimens with PBS or NTsiRNA-PEI and analyzed surface upregulation of costimulatory CD80 as an indicator of tumor DC activation. Supporting our previous findings (10, 13), the most abundant leukocyte subset in these solid tumors were CD45+DEC205+CD3-CD20-CD14- DCs, which on average are composed of a mixed population of 83% CD11b- and 17% CD11b+ cells (Supplemental Figure 3C). Most importantly, as in our mouse model, NTsiRNA-PEI induced a significant increase in the expression of costimulatory CD80 on these cells, compared with those incubated with PBS, in 5 of 6 human specimens (Figure 2D). Supporting these results and confirming the immunostimulatory properties of PEI-
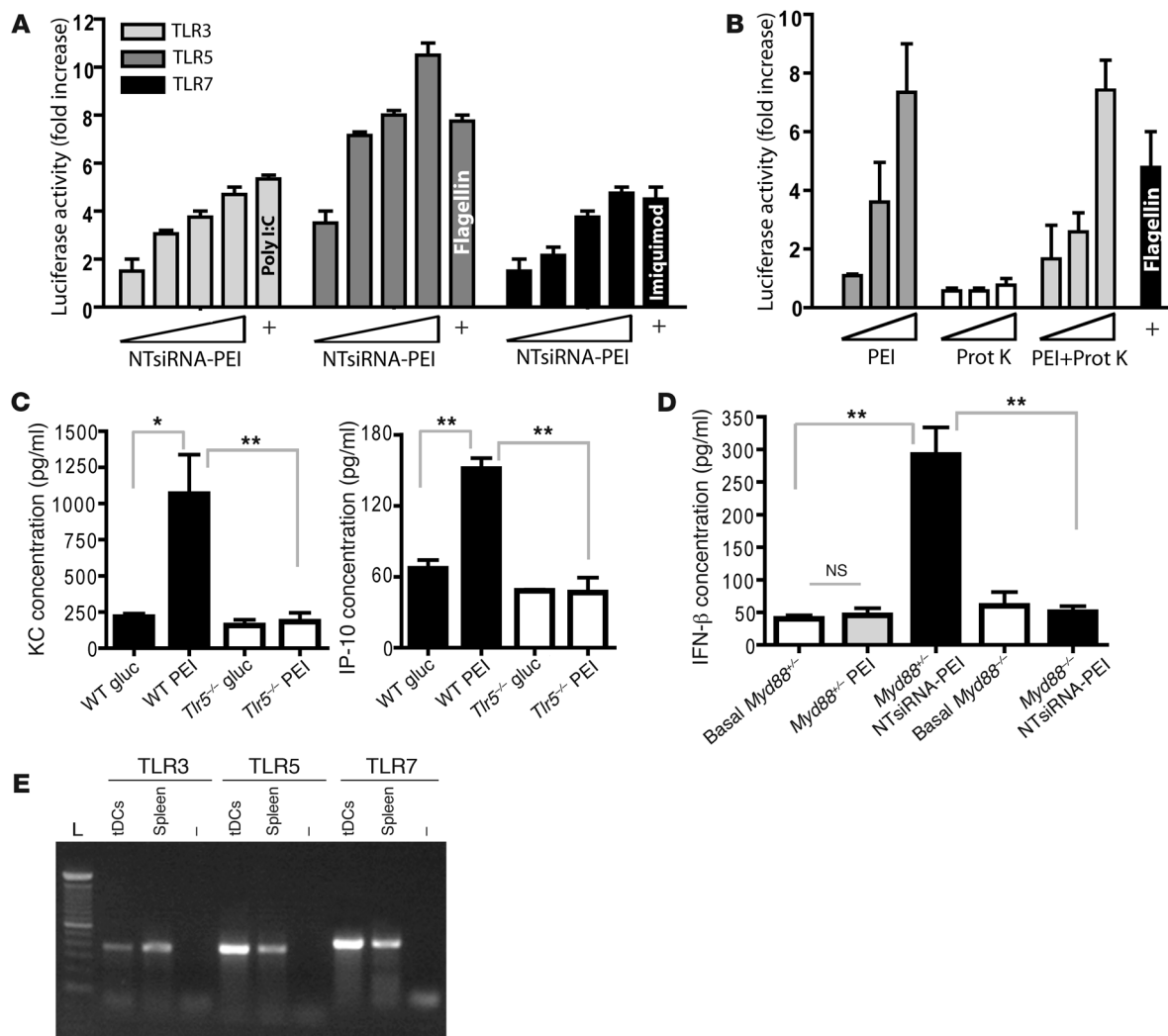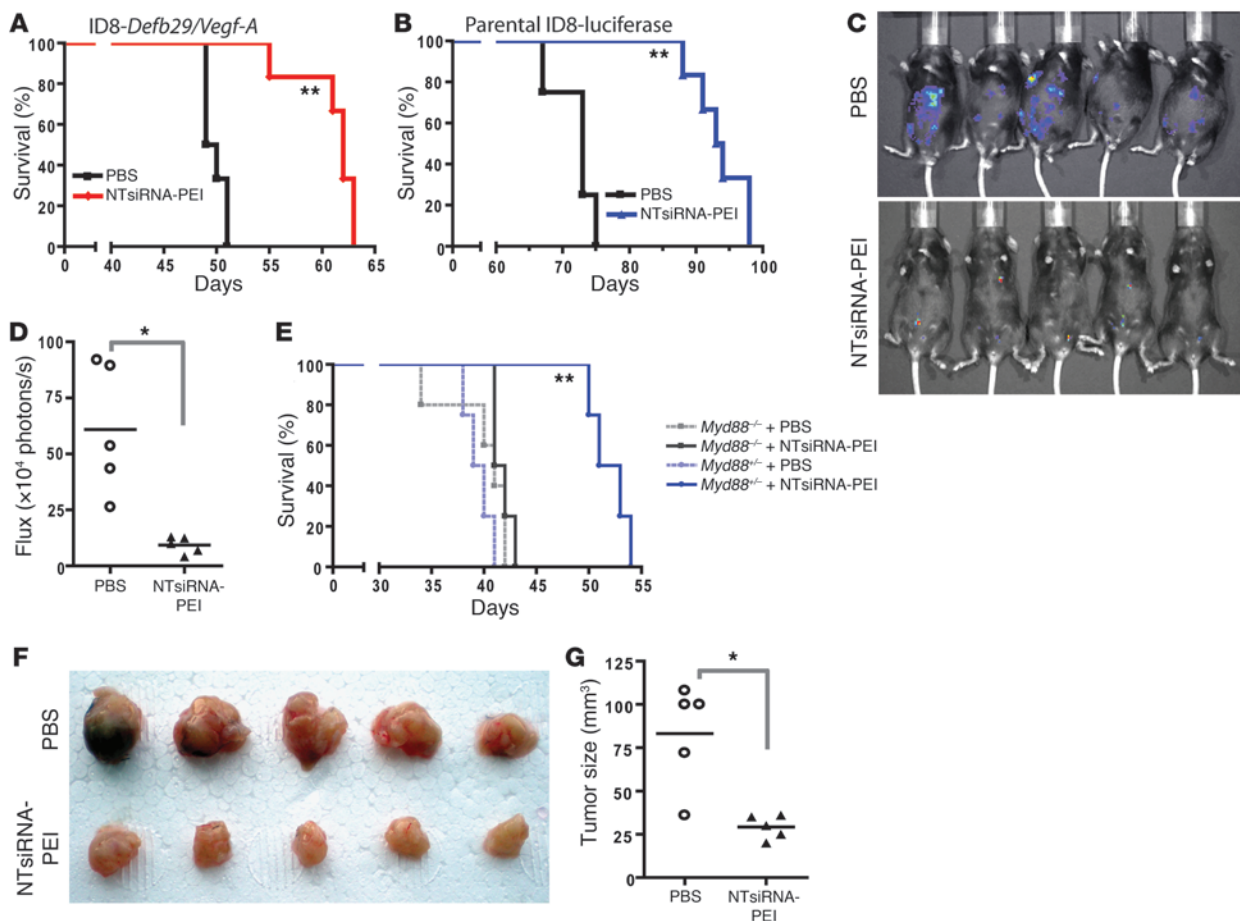
Figure 4
siRNA-PEI nanoparticles stimulate multiple TLRs in vitro and in vivo. (**A**) siRNA-PEI nanocomplexes dose-dependently stimulated TLR3, TLR5, and TLR7 in vitro. Cotransfected HEK293 cells were stimulated with increasing amounts of siRNA-PEI nanoparticles or positive control agonists (+) as described in Methods. Data are representative of 4 independent experiments. (**B**) PEI was sufficient to stimulate TLR5 in vitro in a dose-dependent manner. HEK293 cells expressing TLR5 and harboring an NF-κB–dependent luciferase reporter plasmid were stimulated with increasing amounts of PEI, proteinase K (Prot K), or PEI treated overnight at 55°C with proteinase K (1 mg/ml), and luciferase activity was measured as described in Methods. Data are representative of 3 independent experiments. (**C**) PEI induced rapid cytokine secretion in vivo in a TLR5-dependent manner. Naive WT or $Tlr5^{-/-}$ mice were intraperitoneally injected with 5% glucose (gluc) or linear PEI, and serum levels of KC and IP-10 were determined 2 hours later by cytokine assay (see Methods). Data are representative of 4 mice per group, 2 independent experiments. (**D**) PEI-complexed siRNA induced MyD88-dependent secretion of IFN-β at tumor locations. Ascites from $Myd88^{+/-}$ or $Myd88^{-/-}$ mice bearing advanced ID8-*Defb29/Vegf-A* ovarian tumors were collected prior to (Basal) and 3 hours after intraperitoneal administration of PEI or NTsiRNA-PEI, and levels of IFN-β were analyzed by ELISA. Data are representative of 4 mice per group, 2 independent experiments. (**E**) CD45+CD11c+MHC-II+ tumor DCs were sorted from the peritoneal cavity of mice bearing ID8-*Defb29/Vegf-A* tumors, and TLR expression was confirmed by RT-PCR. Error bars in **A**–**D** denote SEM. *$P < 0.05$; **$P < 0.01$.

ovarian cancer–associated DCs, converting them from a tolerogenic to an efficient antigen-presenting cell type with additional tumor-killing capacity.

Different siRNA-PEI nanoparticle components specifically activate diverse TLRs. The MyD88-dependent maturation of tumor DCs incorporating PEI-based nanocomplexes (Supplemental Figure 3B) suggests a TLR-activating mechanism. To determine whether our nanocomplexes induce TLR signaling, we first used a standard system of HEK293 cells individually expressing each murine TLR

and harboring an NF-κB–dependent luciferase reporter plasmid (29). In support of previous results about naked siRNA (16, 19, 20), oligonucleotides of NTsiRNA-PEI stimulated TLR3 and TLR7 in a dose-dependent manner (Figure 4A). Surprisingly, NTsiRNA-PEI also triggered strong TLR5 activation in a dose-dependent manner (Figure 4A). Because nucleic acids do not stimulate TLR5, we tested the capacity of linear PEI to activate this TLR. Strikingly, PEI was sufficient to stimulate TLR5 in a robust, dose-dependent manner (Figure 4B). PEI did not stimulate membrane-bound

Figure 5
siRNA-PEI nanocomplexes prolong survival in a T cell–mediated, MyD88-dependent manner. (**A** and **B**) Mice bearing aggressive ID8-*Defb29/Vegf-A* (**A**) or luciferase-expressing parental ID8 (**B**) tumors were treated intraperitoneally with PBS or NTsiRNA-PEI nanoparticles at days 8, 13, 18, 23, and 27 after tumor challenge, and survival was monitored over time. Data are representative of 2 independent experiments with a total of 12 mice per group. (**C**) Mice bearing preestablished luciferase-expressing parental ID8 ovarian tumors were intraperitoneally treated with PBS or NTsiRNA-PEI as described above, and luciferin was injected 70 days after tumor challenge to monitor tumor burden in vivo. (**D**) Quantification of the tumor burden shown in **C**. (**E**) Nanoparticle-mediated increase in survival was completely MyD88 dependent. *Myd88*^{+/-} or *Myd88*^{-/-} mice bearing aggressive ID8-*Defb29/Vegf-A* ovarian tumors were treated with PBS or NTsiRNA-PEI as described above, and survival was monitored over time. Data are representative of 2 independent experiments with a total of 10 mice per group. (**F**) Treatment with siRNA-PEI nanocomplexes induced T cell–mediated antitumor protective immunity. CD3+ T cells (3×10^6) purified from the spleens of mice treated with PBS or NTsiRNA-PEI were intravenously transferred into naive C57BL/6 mice previously irradiated with 3 Gy (*n* = 5 per group); after 24 hours, mice were challenged in the flank with ID8-*Defb29/Vegf-A* ovarian carcinoma cells. Tumor pictures were taken 2 months later. (**G**) Quantification of tumor size from **F**. In **D** and **G**, data points and horizontal bars denote individual values and means, respectively. *$P < 0.05$; **$P < 0.01$ versus respective PBS control, log-rank test (**A**, **B**, and **E**) or Mann-Whitney test (**D** and **G**).

TLR2 or endosomal TLR3 and TLR7, indicative of TLR5 specificity (Supplemental Figure 4A). Moreover, TLR5 activation was not caused by contamination of PEI with bacterial or other protein source, as endotoxin was undetectable in the PEI preparation and PEI treated overnight with proteinase K — a procedure that completely ablates the activity of flagellin to activate TLR5 — induced the same dose-dependent TLR5 activation (Figure 4B). In addition, intraperitoneal administration of linear PEI in WT mice, pretreated or not with proteinase K, induced the same serum cytokine secretion pattern reported for flagellin (30), with significant and selective upregulation of keratinocyte chemoattractant (KC) and IFN-inducible protein 10 (IP-10) 2 hours after injection (Figure 4C and Supplemental Figure 4B). Most importantly, PEI-mediated

KC and IP-10 upregulation was completely abrogated in *Tlr5*^{-/-} littermates (Figure 4C), confirming that linear PEI is a TLR5 agonist, which we believe to be novel, with a range of activities similar to those of flagellin.

Furthermore, intraperitoneal injection of NTsiRNA-PEI rapidly induced significant secretion of IFN-β at tumor locations in a completely MyD88-dependent manner (Figure 4D). Because the administration of (TLR5-activating) PEI alone did not affect IFN-β secretion (Figure 4D) and TLR3 signaling is MyD88 independent, this effect should be attributed to the selective stimulation of TLR7 by siRNA in vivo. Importantly, IL-1β, which is processed and secreted in a mature form in response to various proinflammatory stimuli, was not upregulated in the serum of WT mice injected with PEI
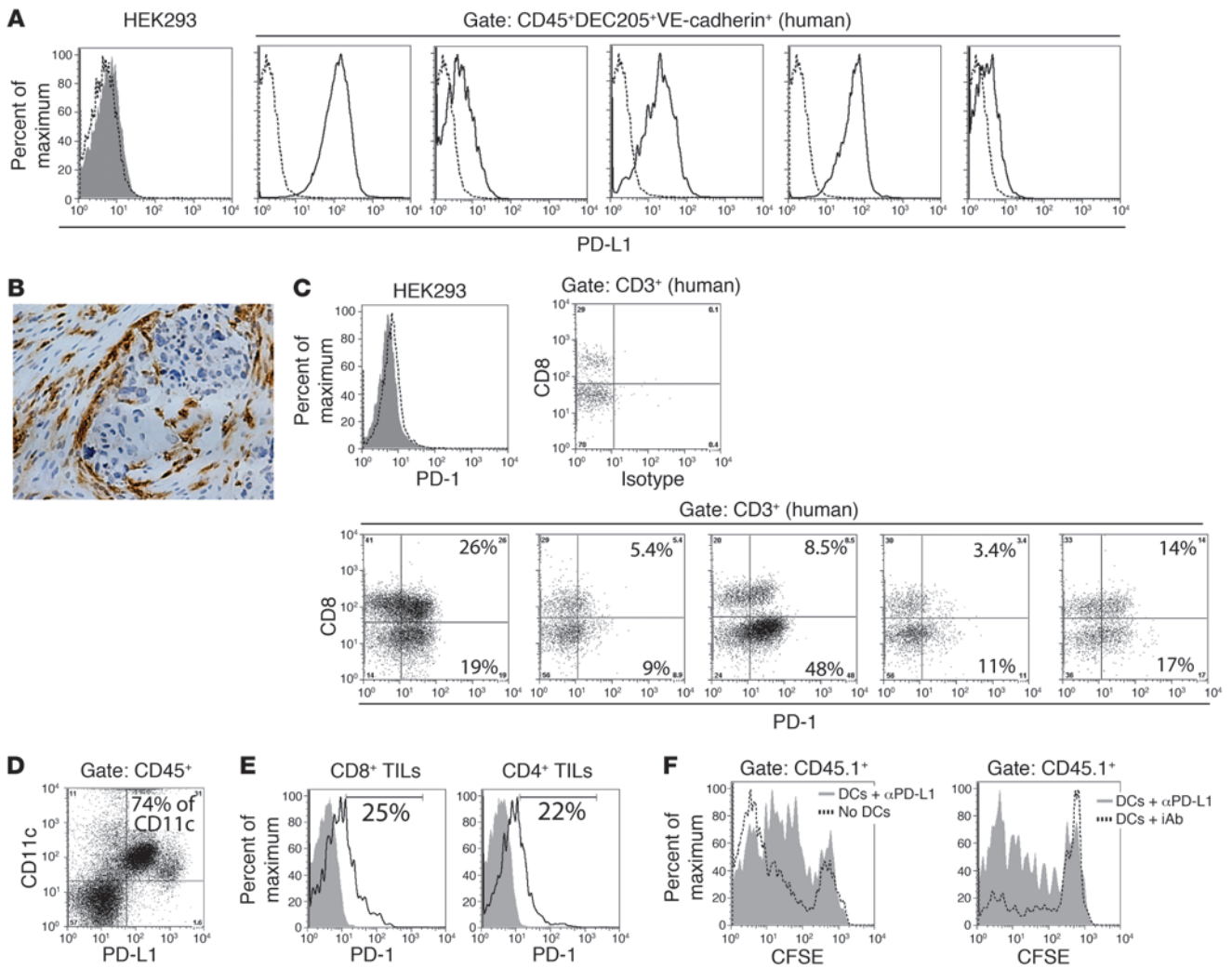
Figure 6

PD-L1 on ovarian cancer–associated DCs inhibits antigen-specific T cell responses. (**A**) FACS analysis of PD-L1 expression on HEK293 cells (negative control) or CD45+DEC205+VE-cadherin+ DCs infiltrating 5 unselected dissociated stage III human tumors. Dotted histograms represent isotype control staining. (**B**) Representative immunohistochemistry of PD-L1+ cells surrounding a tumor islet in a human ovarian carcinoma specimen. Original magnification, ×200. (**C**) PD-1 expression on control HEK293 cells and tumor-infiltrating lymphocytes (TILs) matching the human specimens in **A**. Dotted histogram represents isotype control staining; filled histogram demonstrates negative PD-1 staining. The percentage of human tumor-infiltrating T cells that express PD-1 is indicated. (**D**) PD-L1 expression by peritoneal tumor DCs in mice bearing advanced ID8-*Defb29/Vegf-A* ovarian carcinoma. The percentage of CD11c+ cells coexpressing PD-L1 is indicated. (**E**) Representative FACS analysis of PD-1 expression by T cells infiltrating mouse ID8-*Defb29/Vegf-A* ovarian tumors. Filled histograms indicate isotype control; open histograms show PD-1 staining. The percentage of mouse tumor-infiltrating T cells expressing PD-1 is indicated. (**F**) Representative FACS analyses of mice transferred with PD-L1–blocked DCs compared with both a mouse that did not receive DCs (left) and a mouse transferred with DCs incubated with corresponding isotype control antibodies (iAb; right).

alone or NTsiRNA-PEI (Supplemental Figure 4C), which suggests that the inflammasome does not play a substantial role in the observed immunological effects. Because CD45+CD11c+MHC-II+ DCs sorted from ovarian cancer–bearing mice expressed TLR3, -5, and -7 (Figure 4E), these results suggest that the combined and distinct immunostimulatory activities of linear PEI (through TLR5) and siRNA (mainly through TLR7) converge on tumor-associated DCs to reprogram their tolerogenic phenotype and promote their immunostimulatory potential in vivo and in situ.

siRNA-PEI nanoparticle treatment prolongs survival in a MyD88-dependent, T cell–mediated manner. To determine the therapeutic

potential of using TLR-activating immunostimulatory siRNA-PEI nanoparticles that reprogram tumor-associated regulatory DCs, we next treated mice bearing established aggressive ID8-*Defb29/Vegf-A* ovarian tumors (9) with NTsiRNA-PEI or PBS (n = 12 per group; 2 independent experiments). Treatments started 8 days after tumor challenge and were limited to 4 additional injections on days 13, 18, 23, and 27. Importantly, no obvious toxicity was observed in mice treated with nanocomplexes. Supporting the potential of siRNA-PEI nanoparticles as inherent immunoactivating adjuvants, tumor-bearing mice treated with these nanocomplexes showed a dramatic increase in survival compared with mice
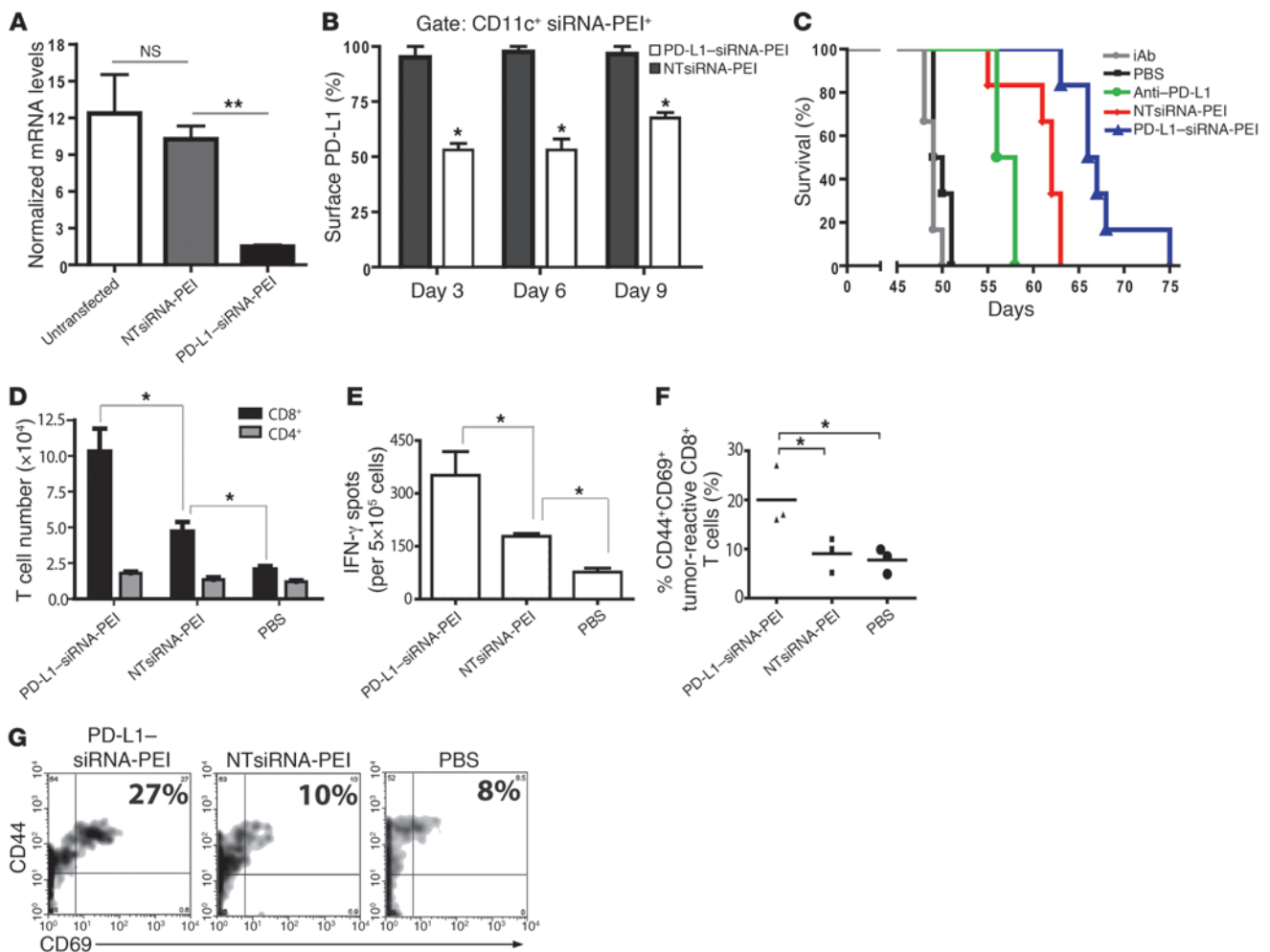
Figure 7
Treatment with PD-L1–siRNA-PEI induces enhanced therapeutic effects. (**A**) Ascites cells from mice bearing ID8-*Defb29/Vegf-A* tumors were left untreated or transfected in vitro with PD-L1–siRNA-PEI or NTsiRNA-PEI, and PD-L1 mRNA levels were measured 48 hours later by real-time RT-PCR. Experiments were repeated 3 times with similar results. (**B**) Silencing PD-L1 on tumor DCs in vivo. Tumor-bearing mice were intraperitoneally injected with rhodamine-labeled PD-L1–siRNA-PEI or NTsiRNA-PEI, and PD-L1 expression in tumor DCs that engulfed the nanocomplexes was determined by FACS. Experiments were repeated twice with similar results. (**C**) Mice bearing aggressive ID8-*Defb29/Vegf-A* tumors were treated intraperitoneally as described in Methods, and survival was monitored over time. Data are representative of 2 independent experiments, 12 mice per group. Significant differences were as follows: anti–PD-L1 versus isotype control antibodies (*P* < 0.05), NTsiRNA-PEI versus PBS (*P* < 0.01), PD-L1–siRNA-PEI versus anti–PD-L1 (*P* < 0.05), and PD-L1–siRNA-PEI versus NTsiRNA-PEI (*P* < 0.05). (**D–G**) Improved antitumor immune responses at tumor locations in mice treated with PD-L1–siRNA-PEI. Tumor-bearing mice (*n* = 3 per group, 3 independent experiments) were treated as described above, and peritoneal wash samples were analyzed at day 27. (**D**) CD4+ and CD8+ T cell infiltration in the peritoneal cavities of treated mice. (**E**) Representative ELISPOT analysis showing increased numbers of IFN-γ–producing cells in mice treated with PD-L1–siRNA-PEI. (**F**) Proportion of activated tumor-specific CD8+ T cells infiltrating the peritoneal cavities of mice. Data points and horizontal bars denote individual values and means, respectively. (**G**) Representative FACS analysis of **F**. The percentage of tumor-reactive CD8+ T cells coexpressing the activation markers CD44 and CD69 is indicated. Error bars in **A**, **B**, **D**, and **E** denote SEM. *P < 0.05; **P < 0.01.

treated with PBS (Figure 5A). Importantly, treatment with these nanoparticles also improved the survival of mice bearing parental ID8 tumors that do not ectopically express *Vegf-A* or *Defb29* (Figure 5B). Correspondingly, we found a significant reduction in tumor burden in mice treated with nanocomplexes compared with control mice (Figure 5, C and D). Therefore, reversing the tolerogenic phenotype of ovarian cancer DCs using intrinsically immunostimulatory siRNA-PEI nanoparticles caused therapeutically relevant responses against lethal ovarian cancers in the absence of specific tumor cell targeting.

Notably, these therapeutically relevant antitumor effects were completely TLR dependent, as treatment with siRNA-PEI nanocomplexes elicited a significant survival increase in *Myd88+/−* heterozygous mice bearing aggressive ovarian cancer, while *Myd88−/−* littermates treated identically failed to respond to the treatment (Figure 5E). Because the increase in survival was entirely abolished in *Myd88−/−* mice, these data further indicate that, in our model, TLR3 stimulation does not play a major role in the therapeutic effects elicited by siRNA-PEI nanocomplexes. Together, these results highlight the intrinsic immunostimulatory potential of
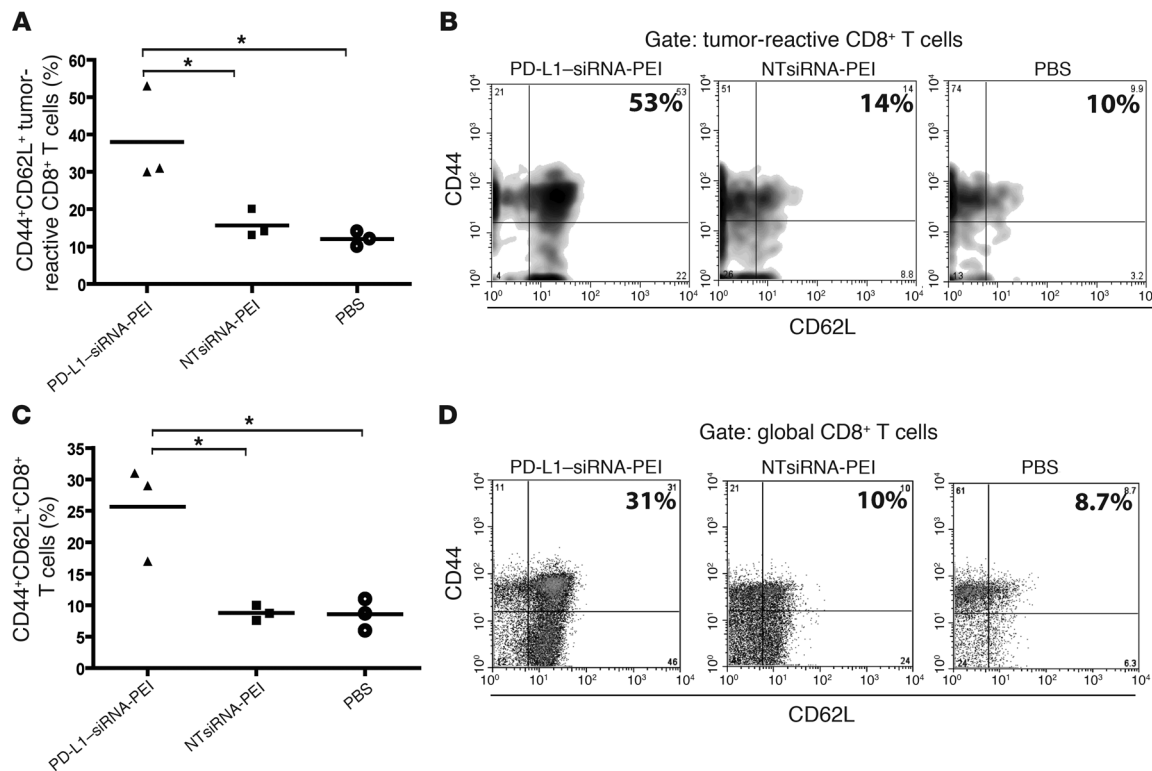
Figure 8
Increased proportion of antitumor central memory–like T cells in the bone marrow of mice treated with PD-L1–siRNA-PEI. (**A**) Percentage of tumor-reactive CD8+ T cells expressing central memory markers in the bone marrow of mice treated with PD-L1–siRNA-PEI. (**B**) Representative FACS analysis of **A**. (**C**) Proportion of global CD8+ T cells exhibiting a central memory–like phenotype in the bone marrow of tumor-bearing mice. Data are representative of 3 independent experiments with similar results. (**D**) Representative FACS analysis of **C**. *$P < 0.05$. In **B** and **D**, the percentage of tumor-reactive or global CD8+ T cells coexpressing the central memory markers CD44 and CD62L is indicated.

TLR-activating siRNA-PEI nanoparticles and their potential for reversing ovarian cancer–induced immunosuppression.

T cells are the only component in the ovarian carcinoma microenvironment capable of exerting spontaneous immune pressure against tumor progression (12, 14, 15). Thus, we next determined whether protective antitumor T cell responses are elicited in response to treatment with siRNA-PEI nanocomplexes. For this purpose, we negatively immunopurified splenic T cells from ID8-*Defb29/Vegf-A* tumor–bearing mice previously treated with PBS or NTsiRNA-PEI. T cells from both groups (3×10^6 cells/mouse) were adoptively transferred into different groups of naive mice, which were challenged 24 hours later with flank ID8-*Defb29/Vegf-A* tumors. As shown in Figure 5, F and G, splenic T cells transferred from tumor-bearing mice treated with siRNA-PEI nanocomplexes induced significant protection against the growth of the same tumors compared with T cells transferred from tumor-bearing mice treated with PBS ($P < 0.05$, Mann-Whitney). Therefore, DCs reeducated at tumor locations by the engulfment of immunostimulatory siRNA-PEI nanoparticles elicited therapeutically relevant T cell–mediated responses that increased survival in ovarian cancer–bearing hosts in a MyD88-dependent (i.e., TLR-dependent) manner.

Tumor-associated DCs suppress antigen-specific immune responses through PD-L1. Since siRNA-PEI nanoparticles reprogrammed tumor regulatory DCs in vivo and in situ in a siRNA sequence–independent manner, we hypothesized that discernible enhanced anti-

tumor immunity along with stronger therapeutic effects could be achieved through sequence-specific silencing of selected immunosuppressive mediators. To define a clinically relevant tolerogenic target, we analyzed the expression of immunosuppressive PD-L1 (3, 7) on CD45+DEC205+VE-cadherin+ DCs infiltrating human solid ovarian carcinoma specimens. Confirming previous observations (10, 13), these canonical DCs expressed MHC-II and CD11c, and to a much lesser extent CD80, but not CD14 or CD11b (data not shown). In support of prior reports (3), most human tumor-infiltrating DCs expressed significant levels of PD-L1, while T cells in matching specimens expressed the PD-1 receptor (Figure 6, A and C). Consistent with the perivascular homing of tumor DCs (10), a barrier of nontumor PD-L1+ cells surrounding tumor islets was found in several human histological sections (Figure 6B).

To confirm the functional relevance of PD-L1 specifically expressed on tumor DCs in vivo, we sorted PD-L1+CD45+CD11c+ VE-cadherin+ DCs from the ascites of mice growing intraperitoneal ID8-*Defb29/Vegf-A* tumors (9). In this aggressive ovarian cancer model, tumor-infiltrating DCs (9), but not tumor cells or other leukocytes, expressed significant levels of PD-L1 (Figure 6D and Supplemental Figure 5A), while cancer-infiltrating T cells expressed the PD-1 receptor (Figure 6E). Thus, we incubated tumor DCs ex vivo with PD-L1–blocking or isotype control antibodies and combined them with magnetically purified, CFSE-labeled, OVA-specific OT-1 CD8+ T cells. These mixed cells were

intraperitoneally injected into mice bearing intraperitoneal OVA-expressing ID8 tumors. An additional group received CFSE-labeled OT-1 CD8+ T cells alone. As expected, OVA-specific T cells proliferated more in the absence of injected PD-L1+ tumor DCs (Figure 6F, left). Furthermore, the expansion of OT-1 T cells admixed with PD-L1–blocked tumor DCs (87.6% ± 4.7% of proliferating cells) was significantly greater than that of OT-1 lymphocytes admixed with DCs incubated with isotype control antibodies (60.4% ± 1.7% of proliferating cells; $P < 0.05$, Mann-Whitney; Figure 6F, right). Therefore, the amount of PD-L1 expressed on tumor-derived DCs was sufficient to prevent the proliferation of transgenic T cells. As ovarian cancer–infiltrating DCs home to perivascular locations (9, 10), these results imply that extravasating PD-1+ antitumor lymphocytes are forced to interact with PD-L1+ DCs, thus abrogating their function before reaching tumor islets. Therefore, we hypothesized that silencing PD-L1 expression on ovarian cancer DCs using PEI-based nanocomplexes containing PD-L1–specific siRNA (PD-L1–siRNA-PEI) could boost endogenous antitumor immune responses and enhance the therapeutic effect of NTsiRNA-PEI.

Treatment with PD-L1–siRNA-PEI induces discernible enhanced antitumor immunity. To silence PD-L1 in tumor DCs, we first defined a siRNA sequence that reduced PD-L1 mRNA levels by about 80% in in vitro transfection experiments of total tumor ascites cells (Figure 7A), and then injected PD-L1–siRNA-PEI into the peritoneal cavity of ovarian carcinoma–bearing mice. As expected, compared with NTsiRNA-PEI, PD-L1–siRNA-PEI reduced the amount of surface PD-L1 on tumor DCs in vivo by approximately 50% 3 days after intraperitoneal administration into mice bearing ID8-*Defb29/Vegf-A* tumors ($P < 0.05$; Figure 7B and Supplemental Figure 5B). Importantly, significant PD-L1 downregulation of about 50% and 33% persisted in situ for 6 and 9 days, respectively (Figure 7B). Therefore, the selective and avid engulfment of siRNA-PEI nanocomplexes by tumor-associated DCs can also be exploited to persistently and specifically downregulate common immunosuppressive mediators, both in vivo and in situ.

To demonstrate that selective silencing of individual genes in vivo results in effects distinguishable from the intrinsic immunostimulation elicited by NTsiRNA-PEI, we treated mice bearing established intraperitoneal ID8-*Defb29/Vegf-A* tumors (n = 12 per group; 2 independent experiments) with either PD-L1–siRNA-PEI or NTsiRNA-PEI, neutralizing PD-L1 or isotype control antibodies, or PBS alone.

As expected, anti–PD-L1 antibody blockade induced a significant survival increase compared with tumor-bearing mice treated with PBS or isotype control antibodies (Figure 7C), supporting the detrimental effects of PD-L1 expression by ovarian cancer–associated DCs. Confirming our results shown above, mice treated with NTsiRNA-PEI exhibited an even greater increase in the median lifespan (Figure 7C). More importantly, delivery of PD-L1–siRNA-PEI induced a further significant increase in survival (Figure 7C). Therefore, while siRNA-PEI nanocomplexes induced therapeutic effects that were independent of PD-L1 targeting, the abrogation of PD-L1 signaling by ovarian cancer–associated DCs — the only cell type that exhibited substantial PD-L1 expression in this model — resulted in discernible enhanced therapeutic benefits.

We next analyzed antitumor immune responses in mice receiving PD-L1–siRNA-PEI. Notably, mice bearing established ID8-*Defb29/Vegf-A* tumors and treated with PD-L1–siRNA-PEI contained significantly more CD8+ T cells in the peritoneal cavity than did mice receiving NTsiRNA-PEI or PBS (Figure 7D). Most importantly, the number of peritoneal T cells producing IFN-γ upon stimulation

with tumor antigens in ELISPOT analyses significantly increased after administration of PD-L1–siRNA-PEI compared with that of mice treated with NTsiRNA-PEI or PBS (Figure 7E). Confirming the requirement of gene-specific silencing for maximal immunotherapeutic efficacy, the percentage of activated (CD69+), antigen-experienced (CD44+) CD8+ T cells specifically recognizing an H-2D^b–restricted mesothelin epitope expressed by ID8 tumor cells (31) in tetramer analyses was significantly higher at tumor locations in mice treated with PD-L1–siRNA-PEI than in mice receiving NTsiRNA-PEI or PBS (Figure 7, F and G). Finally, mice treated with PD-L1–siRNA-PEI — but not NTsiRNA-PEI — showed a greater proportion of mesothelin-specific (i.e., tumor-specific) and total CD8+ T cells displaying attributes of central memory (i.e., CD44+CD62L+) lymphocytes in the bone marrow (Figure 8, A–D), a common reservoir for memory T cells in cancer (32, 33).

Together, these data indicate that treatment with siRNA-PEI nanoparticles elicits therapeutically relevant T cell–mediated responses against ovarian cancer independently of the siRNA sequence and that these effects can be further enhanced when expression of a common immunosuppressive mediator, such as PD-L1, is specifically targeted.

Discussion

Here we demonstrate that PEI-based nanoparticles encapsulating nonviral siRNA are preferentially and avidly engulfed by tumor-associated CD11c+PD-L1+ tolerogenic DCs at ovarian cancer locations. Nanoparticle uptake stimulated multiple TLRs — signaling mainly via MyD88 to transform tumor-resident DCs from an immunosuppressive to an immunostimulatory cell type with enhanced antigen-presenting capacity and direct tumoricidal activity — both in vivo and in situ. Consequently, treatment with siRNA-PEI nanocomplexes resulted in a MyD88-dependent, T cell–mediated increase in survival accompanied by reduced tumor burden.

We found that different components of the siRNA-PEI nanocomplexes activated specific TLRs expressed by tumor-associated DCs. First, supporting previous reports (16, 19, 20), siRNA-carrying nanocomplexes, but not PEI alone, stimulated TLR3 and TLR7 in vitro in a dose-dependent manner; however, the secretion of IFN-β elicited at tumor locations by siRNA-PEI nanoparticles — again, not by PEI alone — was completely MyD88 dependent, indicative of a predominant role for TLR7 over TLR3 on the therapeutic effects. Because PEI is a transfection reagent that facilitates the cellular uptake of externally administered siRNA, TLR7 is likely to be activated at endosomal compartments, and therefore may induce even stronger effects than naked siRNA (17, 18). In the present study, TLR7 was activated by nanocomplexes carrying nontargeting siRNA oligonucleotides, which supports the proposal of Judge and Maclachan that TLR7 recognizes a simple pattern of ribonucleotides (including GU-rich sequences) occurring at high frequency in conventional synthetic siRNA (20). Second, linear PEI, a polymer widely used to deliver nucleic acids in vivo (34–36) and currently used in clinical trials, selectively stimulated TLR5 of mouse and human (our unpublished observations) origin in vitro in a dose-dependent manner and induced the same distinctive pattern of inflammatory cytokines triggered in vivo by flagellin in a TLR5-dependent manner. Although the molecular basis of the interaction between TLR5 and PEI may be unveiled in future studies, it is tempting to speculate that PEI structurally resembles the fragment of monomeric flagellin recognized by TLR5. Thus, we believe our work identifies linear PEI as a novel TLR5 agonist

and indicates that multiple TLR signals, mainly those of TLR7 and TLR5, triggered by siRNA-PEI nanocomplexes converge to activate tumor-associated DCs in situ, reprogramming them in vivo to become efficient antigen-presenting cells.

Interestingly, we found that engulfment of PEI-based nanocomplexes also promoted direct tumoricidal activity by ovarian cancer DCs. Recently, novel subsets of cytotoxic DCs, called killer DCs (KDCs), have been reported (27, 37, 38), although subsequent reports suggested that most KDC-like cells represented NK cells (NK1.1$^+$) upregulating CD11c and MHC-II upon activation (39). Because we specifically sorted NK1.1$^-$CD11c$^+$MHC-II$^+$ cells to prevent NK cell contamination, our results confirmed the cytotoxic potential of DCs against tumor cells. This direct tumoricidal activity should increase tumor antigen availability in vivo and therefore further contribute to cross-presentation of tumor antigens to cytotoxic T lymphocytes and enhanced antitumor immune responses.

Of note, the therapeutic effects in our system were mediated by T cells in a completely MyD88-dependent — and therefore TLR-dependent — manner, a finding substantially different from that of Poeck et al., who report the absence of detectable TLR-dependent immunostimulatory effects for PEI-complexed siRNA in a nonepithelial tumor model (34). Nevertheless, it is possible that DCs specifically recruited to epithelial ovarian cancers, but not B16 tumors, express the adequate combination of TLRs stimulated by siRNA-PEI nanoparticles. Ovarian carcinoma represents an obvious target for siRNA delivery for several other reasons. On the one hand, even as a devastating metastatic disease, ovarian cancer is frequently restricted to the peritoneal cavity, which prevents the need for systemic siRNA administration. On the other hand, ovarian cancer incorporates a large number of targetable immunosuppressive leukocytes with phagocytic and antigen-presenting capacity (3, 9, 10, 13); these include regulatory DCs (9, 10), which have low proliferative capacity, and in which sustained silencing can be achieved because siRNA is not diluted with cell divisions (23). Correspondingly, we found that downregulation of PD-L1 on the surface of tumor DCs engulfing siRNA-PEI nanocomplexes persisted for up to 9 days, which partly explains the increased therapeutic effect against the aggressive ovarian cancer model used compared with the use of PD-L1–blocking antibodies previously proven to be effective in other cancer systems (40, 41).

In addition, ovarian carcinomas have recently emerged as attractive immunotherapeutic targets. First, ovarian cancers express tumor antigens known to be recognized by antibodies and/or CD8$^+$ T cells (42–45). Second, the infiltration of ovarian tumor islets by T cells is a strong independent prognostic factor (12, 14, 15). However, incompletely understood tumor microenvironmental signals restrain this spontaneous immune pressure against ovarian cancer progression (3, 6). In part because of this poor understanding of the peculiarities of the ovarian cancer microenvironment, immunotherapeutic strategies shown to be effective against other cancer types have so far produced disappointing results in ovarian cancer patients (46). We have recently demonstrated that CD11c$^+$DEC205$^+$MHC-II$^+$ DCs that massively infiltrate murine and human ovarian carcinoma specimens represent an important component of the immunosuppressive machinery orchestrated by ovarian tumors (13). The results of the present study now demonstrate that transforming ovarian cancer–associated DCs in vivo from an immunosuppressive to an immunostimulatory and tumoricidal cell type is not only feasible using siRNA-PEI nanocomplexes, but also more effective against aggressive ovarian tumors than our previously reported synergistic effect of standard chemotherapies combined with DC depletion (13).

Notably, NTsiRNA-PEI also induced strong activation in human tumor-infiltrating DCs in multiple dissociated ovarian carcinoma specimens as well as in immature human monocyte-derived DCs. Compared with the exogenous administration of DC-based vaccines, promoting the immunostimulatory ability of tumor-infiltrating DCs in situ offers the theoretical advantage of additionally eradicating this crucial tolerogenic component from the tumor microenvironment, which may also synergize with other immunotherapies. Because both siRNA and linear PEI are being clinically tested, our results provide a mechanistic rationale for future cancer interventions.

While the intrinsic immunostimulatory capacity of siRNA has raised concerns about the consequences of using these molecules in a clinical setting (18), we demonstrated that the inherent capacity of siRNA-PEI nanocomplexes to activate innate immune mechanisms offers a major opportunity to reverse tumor-induced immunosuppression while simultaneously silencing specific genes. In fact, we also achieved specific and persistent downregulation of immunosuppressive genes in vivo in a siRNA sequence–dependent manner, which resulted in superior immunostimulatory and therapeutic effects. Therefore, while siRNA-PEI nanoparticles taken up by tumor phagocytes boosted antitumor immunity in a nonspecific manner, enhanced and discernible responses were elicited by specifically silencing immunosuppressive molecules such as PD-L1. These combined effects can be used to transform tolerogenic phagocytes commonly found in solid tumors into Trojan horses capable of awakening therapeutically relevant endogenous T cell responses in vivo.

Methods

Animals, tissues, and treatments. WT C57BL/6 mice were purchased from the National Cancer Institute, NIH, or from The Jackson Laboratory. All *Tlr5*$^{-/-}$ and *Myd88*$^{-/-}$ mice used in this study were backcrossed at least 8 generations onto C57BL/6 mice. *Tlr5*$^{-/-}$ mice (provided by S. Akira and S. Uematsu, Osaka University, Osaka, Japan; ref. 47) were rederived via embryonic transplant into mice from The Jackson Laboratory to normalize their microflora and make their colitis much milder. Animal experiments were approved by the Institutional Animal Care and Use Committee at Dartmouth Medical School. Stage III–IV human ovarian carcinoma specimens were procured through Research Pathology Services at Dartmouth under a protocol approved by the Committee for the Protection of Human Subjects at Dartmouth-Hitchcock Medical Center (protocol no. CPHS 17702). Single-cell suspensions or cryosections were generated as we have previously described (10).

We generated ID8-*Defb29/Vegf-A* flank or intraperitoneal tumors as described previously (9). Tumor volumes were calculated as $0.5 \times (l \times w^2)$, where l is length and w is width. To generate the ID8-luciferase cell line, parental ID8 cells were transduced 3 times with pFB-neo-Luciferase retroviruses and selected for 10 days with 0.8 mg/ml G418. For visualization of tumor burden, mice were injected with 0.2 ml of 15 mg/ml luciferin (Promega). After 10 minutes, animals were anesthetized with isoflurane and imaged using the IVIS 200 system (Xenogen Corp.). ID8-OVA cells were as previously described (48).

Endotoxin-free rhodamine-labeled and unlabeled in vivo-jetPEI was purchased from PolyPlus Transfection. To generate PD-L1–siRNA-PEI, 50 μg of siRNA specific for the mouse *Pdcd1lg1* mRNA (sense, CCCACAU-AAAAAACAGUUGTT; antisense, CAACUGUUUUUUAUGUGGGTT; *Silencer* in vivo ready; Ambion) were complexed with in vivo–jetPEI at

an N/P ratio of 6, following the recommendations of the manufacturer (PolyPlus Transfection). NTsiRNA-PEI were produced identically, but using a previously validated 21-nt siRNA sequence that does not exhibit significant homology to any rodent or human genomic sequence (*Silencer* Negative Control no. 1 siRNA; Ambion). For in vivo silencing experiments, mice bearing ID8-*Defb29/Vegf-A* tumors for 3 weeks were intraperitoneally injected with rhodamine-labeled PD-L1–siRNA-PEI or NTsiRNA-PEI (50 μg siRNA complexed with rhodamine-labeled in vivo-jetPEI, N/P ratio of 6, per mouse) and the levels of surface PD-L1 on peritoneal tumor–associated DCs that engulfed nanoparticles were determined by flow cytometry 3, 6, and 9 days after injection.

For survival experiments, WT C57BL/6 or gene-deficient mice were intraperitoneally injected with 1×10^6 ID8-luciferase or aggressive ID8-*Defb29/Vegf-A* ovarian carcinoma cells, and mice were treated at days 8, 13, 18, 23, and 27 after tumor challenge with intraperitoneal injections of PBS, irrelevant isotype control (100 μg/mouse), blocking anti-mouse PD-L1 (clone MIH5, 100 μg/mouse; provided by M. Azuma, Tokyo Medical and Dental University, Tokyo, Japan; refs. 49–51) or freshly prepared nanoparticles (50 μg nontargeted siRNA or PD-L1–specific siRNA complexed with in vivo–jetPEI, N/P ratio of 6, per mouse)

Antigen processing. Mice bearing ID8-*Defb29/Vegf-A* tumors were intraperitoneally injected with 250 μg DQ-OVA (Invitrogen); 24 hours later, mice received a single intraperitoneal injection of PBS, NTsiRNA-PEI (50 μg nontargeting siRNA complexed with in vivo–jetPEI, N/P ratio of 6, per mouse) or equivalent amounts of PEI alone (0.9 μmol in vivo–jetPEI in 200 μl glucose 5% per mouse). After 48 hours, the proportion of peritoneal tumor-associated DCs that efficiently processed the probe (FITC⁺) was determined by FACS.

Antigen presentation. Mice bearing ID8-*Defb29/Vegf-A* ovarian tumors for 3 weeks were intraperitoneally injected with full-length endotoxin-free OVA (grade VII; Sigma-Aldrich), and 24 hours later, mice received a single intraperitoneal injection of PBS, rhodamine-labeled PEI (0.9 μmol in vivo–jetPEI in 200 μl glucose 5% per mouse) or rhodamine-labeled NTsiRNA-PEI (50 μg nontargeting siRNA complexed with in vivo–jetPEI, N/P ratio of 6, per mouse). After 48 hours, ordinary CD45⁺CD11c⁺MHC-II⁺ tumor DCs were sorted from the peritoneal cavity of PBS-injected mice, and PEI- or nanoparticle-engulfing tumor DCs were sorted from mice receiving rhodamine-labeled nanocomplexes. Tumor DCs from different groups were cocultured at 1:10 dilution with CFSE-labeled, OVA-specific OT-1 CD8⁺ T cells, and proliferation was analyzed 3 days later.

TLR activation in vitro. TLR stimulation assays were performed as described previously (29). Briefly, 1×10^5 HEK293 cells in 96-well plates were individually transfected using FuGENE6 (Roche) with plasmids encoding murine TLR1–TLR9, plus an NF-κB–inducible luciferase reporter construct at a 10:1 ratio. At 30 hours after transfection, cells were left untreated or stimulated in DMEM that contained increasing concentrations of in vivo–jetPEI alone (ranging from 0.45 to 2 μM) or NTsiRNA-PEI (25–250 ng nontargeting siRNA correspondingly complexed with in vivo–jetPEI, N/P ratio of 6), and luciferase activity was measured in whole-cell lysates 15 hours later using Steady Lite Plus (Perkin Elmer). Positive control TLR agonists were used at the following concentrations: Pam3Cys (TLR2), 0.5 μg/ml; PolyI:C (TLR3), 2 μg/ml; flagellin (TLR5), 1 μg/ml; and imiquimod (TLR7), 5 μg/ml. Data are represented as the fold increase in luciferase activity relative to cotransfected unstimulated cells.

RT-PCR and real-time RT-PCR. Primers for RT-PCR experiments to confirm TLR expression by tumor DCs were as follows: mouse TLR3 (mTLR3) forward, 5′-CTGACAGAACTCGATCTAATGTC-3′ (exon 4); mTLR3 reverse, 5′-AGAGATTCTGGATGCTTGTG-3′ (exon 5); mTLR5 forward, 5′-GAGA-TCTGCCTCAGAGCACCTACG-3′ (exon 2–3 boundary); mTLR5 reverse, 5′-TGGTCAAGTTAGCATACTGGGTCC-3′ (exon 4); mTLR7 forward,

5′-CTCTCTGTCTCAGAGGACTCC-3′; mTLR7 reverse, 5′-TCTTCCA-GATGGTTCAGC-3′. Real-time RT-PCR experiments were performed using SYBR Green (Applied Biosystems) and the following primers: mPD-L1 forward, 5′-TTCAGATCACAGACGTCAAGCTG-3′; mPD-L1 reverse, 5′-ATTCTCTGGTTGATTTTGCGGTA-3′; mTRAIL forward, 5′-GAGGCAACTGTATCAGCTCATTG-3′; mTRAIL reverse, 5′-GAGCTGC-CACTTTCTGAGGTC-3′; mGAPDH forward, 5′-CCTGCACCACCAACT-GCTTA-3′; mGAPDH reverse, 5′-CATGAGTCCTTCCACGATACCA-3′.

Cytotoxicity assays. Lysis of ID8-*Defb29/Vegf-A* tumor target cells by tumor DCs was determined by a ⁵¹Cr release assay, as previously described (52). For 4 weeks, ID8-*Defb29/Vegf-A* tumor–bearing mice received a single intraperitoneal injection of PBS, PEI alone, or NTsiRNA-PEI as described above, and 36 hours later, CD11c⁺MHC-II⁺CD3⁻NK1.1⁻ tumor-associated DCs were sorted from peritoneal washes (10 ml PBS) and incubated with ⁵¹Cr-labeled ID8-*Defb29/Vegf-A* cells at effector/target ratios of 25:1, 5:1, and 1:1, as indicated, for 5 hours.

ELISPOT. Flat-bottomed, 96-well nitrocellulose-lined plates (Millipore) were coated with IFN-γ mAb (AN-18; eBioscience) and incubated overnight at 4°C. After washing with Coating Buffer (eBioscience), plates were blocked with 10% FBS serum for 2 hours at 37°C. Ficoll-enriched leukocytes (5×10^5 cells), obtained from peritoneal washes (10 ml) of ID8-*Defb29/Vegf-A* tumor–bearing mice treated with siRNA-PEI nanoparticles or PBS at days 8, 13, 18, and 23 after tumor challenge, were cocultured for 72 hours in 10% FBS RPMI medium with 5×10^4 bone marrow–derived DCs previously pulsed overnight with irradiated ID8-*Defb29/Vegf-A* cells. After incubation, plates were washed with 0.05% Tween 20 in PBS, and biotinylated secondary IFN-γ mAb (R4-6A2; eBioscience) was added. After incubation for 2 hours at 37°C, the plates were washed and developed with Avidin–horseradish peroxidase (eBioscience) for 1 hour at room temperature. After washing, fresh substrate (3-amino-9-ethyl carbazole; Sigma-Aldrich) was added, and the plates were incubated for approximately 20 minutes.

Flow cytometry and cytokine assay. Flow cytometry was performed on a FACS-Canto system (BD Biosciences). Cell populations were sorted from peritoneal washes (10 ml PBS) of ovarian carcinoma–bearing mice or from human tumor single-cell suspensions using a FACSAria sorter (BD Biosciences).

Anti-mouse antibodies were specific for CD45 (30-F11), PD-L1 (MIH5), CD69 (H1.2F3), CD11c (HL3; all from BD Biosciences); VE-cadherin (Medsystems Diagnostics); DEC205 (NLDC145; Serotec), and MHC-II (NIMR-4; eBioscience). Anti-human antibodies were specific for CD45 (HI30), DEC205 (MG38), CD3 (UCHT1), CD4 (OKT4), CD8 (RPA-T8), CD31 (M89D3), CD11b (ICRF44), CD14 (M5E2), PD-L1 (MIH1), and PD-1 (MIH4; all from BD Biosciences). Cytokines induced in the serum or ascites of WT or gene-deficient mice upon intraperitoneal injection of PEI (0.9 μmol in vivo–jetPEI diluted in 200 μl glucose 5%) or NTsiRNA-PEI (50 μg nontargeting siRNA complexed with in vivo–jetPEI, N/P ratio of 6) were detected by ELISA or using a Mouse-23-Plex panel cytokine assay (Bio-Rad), following manufacturer's instructions.

Statistics. Differences between the means of experimental groups were analyzed using the Mann-Whitney test. Mouse survival data were analyzed with the log-rank test. Data analysis was performed using Prism software (version 4.0; GraphPad). A *P* value less than 0.05 was considered significant.

Acknowledgments

Address correspondence to: Jose R. Conejo-Garcia, 640W Borwell, HB 7556, 1 Medical Center Drive, Lebanon, New Hampshire 03766, USA. Phone: (603) 650-6822; Fax: (603) 650-6223; E-mail: jose.r.conejo-garcia@dartmouth.edu.

1. Jemal, A., et al. 2008. Cancer statistics, 2008. *CA Cancer J. Clin.* **58**:71–96.
2. Coukos, G., Conejo-Garcia, J.R., Buckanovich, R., and Benencia, F. 2007. Vascular leukocytes: a population with angiogenic and immunossuppressive properties highly represented in ovarian cancer. *Adv. Exp. Med. Biol.* **590**:185–193.
3. Curiel, T.J., et al. 2003. Blockade of B7-H1 improves myeloid dendritic cell-mediated antitumor immunity. *Nat. Med.* **9**:562–567.
4. Gabrilovich, D.I., et al. 2007. The terminology issue for myeloid-derived suppressor cells. *Cancer Res.* **67**:425; author reply 426.
5. Plate, J.M., and Harris, J.E. 2000. Immune cell functions in pancreatic cancer. *Crit. Rev. Immunol.* **20**:375–392.
6. Curiel, T.J., et al. 2004. Specific recruitment of regulatory T cells in ovarian carcinoma fosters immune privilege and predicts reduced survival. *Nat. Med.* **10**:942–949.
7. Keir, M.E., Butte, M.J., Freeman, G.J., and Sharpe, A.H. 2008. PD-1 and its ligands in tolerance and immunity. *Annu. Rev. Immunol.* **26**:677–704.
8. Bak, S.P., Walters, J.J., Takeya, M., Conejo-Garcia, J.R., and Berwin, B.L. 2007. Scavenger receptor-A-targeted leukocyte depletion inhibits peritoneal ovarian tumor progression. *Cancer Res.* **67**:4783–4789.
9. Conejo-Garcia, J.R., et al. 2004. Tumor-infiltrating dendritic cell precursors recruited by a beta-defensin contribute to vasculogenesis under the influence of Vegf-A. *Nat. Med.* **10**:950–958.
10. Conejo-Garcia, J.R., et al. 2005. Vascular leukocytes contribute to tumor vascularization. *Blood.* **105**:679–681.
11. Coukos, G., Benencia, F., Buckanovich, R.J., and Conejo-Garcia, J.R. 2005. The role of dendritic cell precursors in tumour vasculogenesis. *Br. J. Cancer.* **92**:1182–1187.
12. Coukos, G., Conejo-Garcia, J.R., Roden, R.B., and Wu, T.C. 2005. Immunotherapy for gynaecological malignancies. *Expert Opin. Biol. Ther.* **5**:1193–1210.
13. Huarte, E., et al. 2008. Depletion of dendritic cells delays ovarian cancer progression by boosting antitumor immunity. *Cancer Res.* **68**:7684–7691.
14. Zhang, L., et al. 2003. Intratumoral T cells, recurrence, and survival in epithelial ovarian cancer. *N. Engl. J. Med.* **348**:203–213.
15. Conejo-Garcia, J.R., et al. 2004. Ovarian carcinoma expresses the NKG2D ligand Letal and promotes the survival and expansion of CD28- antitumor T cells. *Cancer Res.* **64**:2175–2182.
16. Hornung, V., et al. 2005. Sequence-specific potent induction of IFN-alpha by short interfering RNA in plasmacytoid dendritic cells through TLR7. *Nat. Med.* **11**:263–270.
17. Kleinman, M.E., et al. 2008. Sequence- and target-independent angiogenesis suppression by siRNA via TLR3. *Nature.* **452**:591–597.
18. Rossi, J., Zamore, P., and Kay, M.A. 2008. Wandering eye for RNAi. *Nat. Med.* **14**:611.

19. Marques, J.T., and Williams, B.R. 2005. Activation of the mammalian immune system by siRNAs. *Nat. Biotechnol.* **23**:1399–1405.
20. Judge, A.D., et al. 2005. Sequence-dependent stimulation of the mammalian innate immune response by synthetic siRNA. *Nat. Biotechnol.* **23**:457–462.
21. Hwang, J.Y., et al. 2008. Clinical and biological significance of tissue transglutaminase in ovarian carcinoma. *Cancer Res.* **68**:5849–5858.
22. Merritt, W.M., et al. 2008. Effect of interleukin-8 gene silencing with liposome-encapsulated small interfering RNA on ovarian cancer cell growth. *J. Natl. Cancer Inst.* **100**:359–372.
23. Landen, C.N., Jr., et al. 2005. Therapeutic EphA2 gene targeting in vivo using neutral liposomal small interfering RNA delivery. *Cancer Res.* **65**:6910–6918.
24. Song, E., et al. 2003. Sustained small interfering RNA-mediated human immunodeficiency virus type 1 inhibition in primary macrophages. *J. Virol.* **77**:7174–7181.
25. Grzelinski, M., et al. 2006. RNA interference-mediated gene silencing of pleiotrophin through polyethylenimine-complexed small interfering RNAs in vivo exerts antitumoral effects in glioblastoma xenografts. *Hum. Gene Ther.* **17**:751–766.
26. Urban-Klein, B., Werth, S., Abuharbeid, S., Czubayko, F., and Aigner, A. 2005. RNAi-mediated gene-targeting through systemic application of polyethylenimine (PEI)-complexed siRNA in vivo. *Gene Ther.* **12**:461–466.
27. Stary, G., et al. 2007. Tumoricidal activity of TLR7/8-activated inflammatory dendritic cells. *J. Exp. Med.* **204**:1441–1451.
28. Roux, S., et al. 2008. CD4+CD25+ Tregs control the TRAIL-dependent cytotoxicity of tumor-infiltrating DCs in rodent models of colon cancer. *J. Clin. Invest.* **118**:3751–3761.
29. Gorden, K.B., et al. 2005. Synthetic TLR agonists reveal functional differences between human TLR7 and TLR8. *J. Immunol.* **174**:1259–1268.
30. Vijay-Kumar, M., et al. 2008. Flagellin treatment protects against chemicals, bacteria, viruses, and radiation. *J. Immunol.* **180**:8280–8285.
31. Hung, C.F., Tsai, Y.C., He, L., and Wu, T.C. 2007. Control of mesothelin-expressing ovarian cancer using adoptive transfer of mesothelin peptide-specific CD8+ T cells. *Gene Ther.* **14**:921–929.
32. Di Rosa, F., and Pabst, R. 2005. The bone marrow: a nest for migratory memory T cells. *Trends Immunol.* **26**:360–366.
33. Parretta, E., et al. 2005. CD8 cell division maintaining cytotoxic memory occurs predominantly in the bone marrow. *J. Immunol.* **174**:7654–7664.
34. Poeck, H., et al. 2008. 5′-Triphosphate-siRNA: turning gene silencing and Rig-I activation against melanoma. *Nat. Med.* **14**:1256–1263.
35. Louis, M.H., et al. 2006. Intraperitoneal linear polyethylenimine (L-PEI)-mediated gene delivery to ovarian carcinoma nodes in mice. *Cancer Gene Ther.* **13**:367–374.

36. Zou, S.M., Erbacher, P., Remy, J.S., and Behr, J.P. 2000. Systemic linear polyethylenimine (L-PEI)-mediated gene delivery in the mouse. *J. Gene Med.* **2**:128–134.
37. Taieb, J., et al. 2006. A novel dendritic cell subset involved in tumor immunosurveillance. *Nat. Med.* **12**:214–219.
38. Chan, C.W., et al. 2006. Interferon-producing killer dendritic cells provide a link between innate and adaptive immunity. *Nat. Med.* **12**:207–213.
39. Vosshenrich, C.A., et al. 2007. CD11cloB220+ interferon-producing killer dendritic cells are activated natural killer cells. *J. Exp. Med.* **204**:2569–2578.
40. Saudemont, A., and Quesnel, B. 2004. In a model of tumor dormancy, long-term persistent leukemic cells have increased B7-H1 and B7.1 expression and resist CTL-mediated lysis. *Blood.* **104**:2124–2133.
41. Wei, S., et al. 2008. Tumor-induced immune suppression of in vivo effector T-cell priming is mediated by the B7-H1/PD-1 axis and transforming growth factor beta. *Cancer Res.* **68**:5432–5438.
42. Ramakrishna, V., et al. 2003. Naturally occurring peptides associated with HLA-A2 in ovarian cancer cell lines identified by mass spectrometry are targets of HLA-A2-restricted cytotoxic T cells. *Int. Immunol.* **15**:751–763.
43. Yen, M.J., et al. 2006. Diffuse mesothelin expression correlates with prolonged patient survival in ovarian serous carcinoma. *Clin. Cancer Res.* **12**:827–831.
44. Odunsi, K., et al. 2003. NY-ESO-1 and LAGE-1 cancer-testis antigens are potential targets for immunotherapy in epithelial ovarian cancer. *Cancer Res.* **63**:6076–6083.
45. Hasegawa, K., et al. 2004. SSX expression in gynecological cancers and antibody response in patients. *Cancer Immun.* **4**:16.
46. Kershaw, M.H., et al. 2006. A phase I study on adoptive immunotherapy using gene-modified T cells for ovarian cancer. *Clin. Cancer Res.* **12**:6106–6115.
47. Uematsu, S., et al. 2006. Detection of pathogenic intestinal bacteria by Toll-like receptor 5 on intestinal CD11c+ lamina propria cells. *Nat. Immunol.* **7**:868–874.
48. Barber, M.A., Zhang, T., Gagne, B.A., and Sentman, C.L. 2007. NK cells negatively regulate antigen presentation and tumor-specific CTLs in a syngeneic lymphoma model. *J. Immunol.* **178**:6140–6147.
49. Yamazaki, T., et al. 2002. Expression of programmed death 1 ligands by murine T cells and APC. *J. Immunol.* **169**:5538–5545.
50. Tsushima, F., et al. 2003. Preferential contribution of B7-H1 to programmed death-1-mediated regulation of hapten-specific allergic inflammatory responses. *Eur. J. Immunol.* **33**:2773–2782.
51. Tsushima, F., et al. 2006. Predominant expression of B7-H1 and its immunoregulatory roles in oral squamous cell carcinoma. *Oral Oncol.* **42**:268–274.
52. Barber, A., et al. 2007. Chimeric NKG2D receptor-bearing T cells as immunotherapy for ovarian cancer. *Cancer Res.* **67**:5003–5008.